frontiers | Frontiers in Pharmacology

TYPE Original Research
PUBLISHED 31 March 2023
DOI 10.3389/fphar.2023.1116073

OPEN ACCESS

EDITED BY
Zhihao Liu,
Dalian Medical University, China

REVIEWED BY
Yukuang Guo,
Takeda Oncology, United States
Huang Kai,
Wuxi People's Hospital Affiliated to Nanjing Medical University, China

*CORRESPONDENCE
Dafang Zhong,
dfzhong@simm.ac.cn
Xingxing Diao,
xxdiao@simm.ac.cn
Liyan Miao,
miaolysuzhou@163.com

†These authors have contributed equally to this work

SPECIALTY SECTION
This article was submitted to Drug Metabolism and Transport, a section of the journal Frontiers in Pharmacology

RECEIVED 05 December 2022
ACCEPTED 23 March 2023
PUBLISHED 31 March 2023

CITATION
Zhang H, Yan S, Zhan Y, Ma S, Bian Y, Li S, Tian J, Li G, Zhong D, Diao X and Miao L (2023), A mass balance study of [^{14}C] SHR6390 (dalpiciclib), a selective and potent CDK4/6 inhibitor in humans. *Front. Pharmacol.* 14:1116073. doi: 10.3389/fphar.2023.1116073

A mass balance study of [^{14}C] SHR6390 (dalpiciclib), a selective and potent CDK4/6 inhibitor in humans

Hua Zhang[1,2†], Shu Yan[3†], Yan Zhan[3], Sheng Ma[1,2], Yicong Bian[1,2], Shaorong Li[4], Junjun Tian[3], Guangze Li[4], Dafang Zhong[3*], Xingxing Diao[3*] and Liyan Miao[1,2*]

[1]Department of Clinical Pharmacology, The First Affiliated Hospital of Soochow University, Suzhou, China, [2]Institute for Interdisciplinary Drug Research and Translational Sciences, Soochow University, Suzhou, China, [3]Shanghai Institute of Materia Medica, Chinese Academy of Sciences, Shanghai, China, [4]Jiangsu Hengrui Medicine Co., Ltd., Lianyungang, Jiangsu, China

SHR6390 (dalpiciclib) is a selective and effective cyclin-dependent kinase (CDK) 4/6 inhibitor and an effective cancer therapeutic agent. On 31 December 2021, the new drug application was approved by National Medical Product Administration (NMPA). The metabolism, mass balance, and pharmacokinetics of SHR6390 in 6 healthy Chinese male subjects after a single oral dose of 150 mg [^{14}C]SHR6390 (150 μCi) in this research. The *Tmax* of SHR6390 was 3.00 h. In plasma, the $t_{1/2}$ of SHR6390 and its relative components was approximately 17.50 h. The radioactivity B/P (blood-to-plasma) $AUC_{0\text{-}t}$ ratio was 1.81, indicating the preferential distribution of drug-related substances in blood cells. At 312 h after administration, the average cumulative excretion of radioactivity was 94.63% of the dose, including 22.69% in urine and 71.93% in stool. Thirteen metabolites were identified. In plasma, because of the low level of radioactivity, only SHR6390 was detected in pooled $AUC_{0\text{-}24\ h}$ plasma. Stool SHR6390 was the main component in urine and stool. Five metabolites were identified in urine, and 12 metabolites were identified in stool. Overall, faecal clearance is the main method of excretion.

KEYWORDS

SHR6390, [^{14}C]SHR6390, radioactivity, drug metabolism, CDK, pharmacokinetics

1 Introduction

The disorder of cell division, which leads to abnormal cell proliferation, is one of the key signs of cancer. In cancer treatment, the target of blocking cell division is a very important research goal. Cell cycle usually refers to the stage in which cells pass through a predetermined number of stages under the control of a complex network of regulators (Hartwell et al., 1974). The cell cycle consists of several different stages (Malumbres and Barbacid, 2001). The initiation of cell cycle requires the induction of cyclin and cyclin dependent kinases (CDKs) expression through growth factors, estrogen and other mitogenic stimuli (de Dueñas et al., 2018). Breast cancer is associated with the imbalance of D-cyclin dependent kinase 4/6-retinoblastoma (cyclin D-CDK4/6-retinoblastoma) pathway (Arnold and Papanikolaou, 2005; Cancer Genome Atlas Network, 2012; Witkiewicz and Knudsen, 2014). Class D cyclins (D1, D2 and D3) are regulators of CDK4 and CDK6 kinases, and together form active complexes (Weinberg, 1995). Among them, CDK4/6 manages the

process of cell cycle through reversible binding with cyclin D1. At the early stage of G1, active CDK4 and CDK6 phosphorylate retinoblastoma (RB) protein (a tumor inhibitor), leading to partial release of E2F transcription factor, and then promoting the transcription of downstream genes required to enter S phase through G1 restriction point (Morgan, 1997; Lundberg and Weinberg, 1998). P16 is an endogenous CDK4 inhibitor, which plays a role in reducing cell cycle and is often expressed as loss in malignant tumors (Bartkova et al., 1996). A key feature of tumorigenesis is the uncontrolled proliferation of cells, which is due to the disorder of cell cycle regulation. Therefore, cyclin D1-CDK4/6-RB pathway is a good target for anticancer drugs (Long et al., 2019).

First-generation CDK inhibitors are non-selective universal CDK blockers with limited antitumour activity and obvious toxicity (Shapiro, 2006). More recently, in the treatment of metastatic breast cancer, selective small molecule CDK4/6 inhibitors have also become increasingly effective, such as palbociclib, ribociclib and abemaciclib, which have been developed in metastatic luminal breast cancer (Cadoo et al., 2014). Three CDK4/6 inhibitors, Palbicilib, Ribocib and Abemacilib, which were previously marketed. The chemical structures of Palbicilib and ribocib are similar and have good selectivity. Abemachilib is different from them in structure. Its structure can inhibit other kinases, such as CDK9 (Gelbert et al., 2014). In addition, these CDK4/6 inhibitors show differences in terms of toxicity, so they correspond to different administration schemes. Palbociclib and ribociclib induce bone marrow suppression, which is usually administered for 1 week to restore the neutrophil count in patients, whereas abemaciclib is dosed continuously and elicits fatigue and diarrhoea as more relevant dose-limiting toxicities (Asghar et al., 2015).

SHR6390 (dalpiciclib) is a selective and effective cyclin-dependent kinase (CDK) 4/6 inhibitor and an effective cancer therapeutic agent. On 31 December 2021, the new drug application was approved by NMPA (National Medical Product Administration). SHR6390 exhibited potent antiproliferative activity against a wide range of human RB-positive tumor cells, and exclusively induced G1 arrest as well as cellular senescence, with a concomitant reduction in the levels of Ser780-phosphorylated RB protein. Although many research results on SHR6390 have been published, there are still many problems of concern that have not been solved or disclosed (Wang et al., 2017; Long et al., 2019; Chen et al., 2020; Zhang et al., 2021). To date, there are no data to evaluate its overall metabolism in humans. It is very important to understand the metabolism of SHR6390 through radioactive substances so as to evaluate its safety in the future (Robison and Jacobs, 2009; Penner et al., 2012; Prakash et al., 2019). This research can also help guide the clinical evaluation of SHR6390 in the future and help to select the appropriate dose. The use of radioactive tracers in pharmacokinetic studies enables us to better understand the excretion pathway and metabolism of drugs (Murai et al., 2014; Lappin, 2015; Meng et al., 2019; Yamada et al., 2019; Tian et al., 2021; Zheng et al., 2021). Therefore, in this study, the pharmacokinetics, biotransformation pathway and mass balance of [^{14}C]SHR6390 in humans were investigated.

2 Materials and methods

2.1 Chemicals and reagents

SHR6390 (purity 99.50%) was provided by Jiangsu Hengrui Medicine Co., Ltd. (Lianyungang, China). [^{14}C]SHR6390 (150 μCi, purity 98.62%) and SHR6390 (150 mg) were dissolved in 5% carboxymethylcellulose sodium (CMC-Na, purchased from Aladdin, Shanghai, China) and stored at approximately −20°C. For other reagent information, please refer to another article in our group (Zheng et al., 2021).

2.2 Instruments

High-resolution mass spectrometry (HR-MS) and HR-MS^2 acquisition are currently widely used in the field of metabolite identification, while background subtraction and mass loss filtering techniques have promoted the development of metabolite identification (Zhang et al., 2008; Zhang et al., 2009; Ming Yao et al., 2020). In this study, data are collected through the XCalibur and Laura systems. A Vanquish Ultra High Performance Liquid Chromatography (UHPLC) system was used to carry out detection with a Q Executive Plus mass spectrometer (Thermo, MA, United States). The system setting are shown in Table 1. The mass spectrum data were analysed using Compound Discoverer software (Themo).

2.3 Design, subjects and sample collection

The clinical trial (No. CTR20230830) was an open-label, single-center, single-dose trial conducted at the First Affiliated Hospital of Soochow University (Suzhou, China). This study was conducted in accordance with the ethical principles required by the Helsinki Declaration and approved by the Hospital Ethics Committee (2020. No.151). Six healthy Chinese male subjects were recruited between 18 and 45 years old with a body mass index between 19 and 26 kg/m^2. All subjects signed a written ICF (informed consent form) before the start of the study. Plasma samples were collected from pre-dose to 144 h after dose. Urine and stool samples were collected pre-dose to 312 h after dose administration. The standards of subject out were the following three criteria: The cumulative excretion radioactivity exceeded 80% of the dose radioactivity; the radioactivity excreted was less than 1% of the radioactivity administration over a 24 h period on two consecutive days; and the measured radioactivity in the collected plasma was 3 times lower than that of the pre-dose (Bian et al., 2021). Fasting for at least 10 h and then water deprivation for 1 h, each subject was given a single oral dose of 150 mg [^{14}C]SHR6390 (150 μCi) suspension. Rinse the dosing bottle with warm water and give it to the subjects. The total volume of drug preparation and lotion did not exceed 240 mL. After taking the medicine, the subjects fasted for 4 h and refrained from water for 1 h after dosing. Twenty millilitres of whole blood was collected before administration and 2, 6, 10, 24 and 48 h after administration. In 20 mL of whole blood, 1.6 mL was used for the test, and 0.4 mL was placed in the backup tube. Centrifuge (3,500 rpm, 5 min, 4°C) 10 mL of whole blood to produce plasma. The volume of plasma in one of the two tubes was 3.2 mL, and the remaining plasma was put into the backup tube. The

TABLE 1 UHPLC-HRMS setting.

UHPLC condition		
Colume	ACQUITY UPLC HSS T3 (100 mm × 2.1 mm, 1.8 μm, Waters, United States)	
Phase A	5 mM ammonium acetate aqueous solution	
Phase B	Acetonitrile	
UV detection	254 nm	
Gradient elution	time (min)	B (%)
	0	10
	2	10
	24	30
	26	95
	28.8	95
	28.9	10
	35	10
MS condition		
Source	ESI	
Mode	Positive	
Scan range	100–1,000 Da	
Sheath gas	45 L/min	
Aux gas	10 L/min	
Capillary temperature	320°C	
Capillary voltage	3.5 kV	

remaining 8 mL whole blood was centrifuged (3,500 rpm, 5 min, 4°C) to produce plasma for metabolic study. Meanwhile, 10 mL whole blood was collected at 0.5, 1, 3, 4, 8, 72, 96, 120, and 144 h. The plasma required for detection is obtained by whole blood centrifugation. In addition to collecting urine samples before administration and 0–4 h, 4–8 h, 8–12 h and 12–24 h after administration, urine samples will be collected every 24 h in the following collection periods. Collection of fecal samples, except before administration, shall be conducted at 24-h intervals after administration. Plasma samples were stored at −80°C, and urine and stool samples were stored at −20°C until analysis.

2.4 Radioactivity

The radioactivity of urine and plasma was detected by liquid scintillation counter (LSC) (Tri-Carb 3110 TR, PerkinElmer, MA, United States). Two times the weight of acetonitrile-water (1:1, *v*: *v*) was added to the stool and homogenized. Blood and stool homogenate were weighed and burned in a biological oxidizer (OX-501, Harvey, NY, United States). Then, the CO_2 with 14C labled was trapped in the liquid scintillation cocktail (RDC, NJ, United States) and detected by LSC.

2.5 Radioprofiling

2.5.1 Recovery

The total extraction recovery was 119%, 84.69% and 116.64% in plasma, urine and feces, respectively. The colume recovery was 92.21%, 100.14%, 99.13% in plasma, urine and feces, respectively. The recovery improved the method of extraction and LC-MS was suitable.

2.5.2 Plasma

According to the AUC principle, the plasma of 6 subjects from 0–24 h was pooled (Hop et al., 1998). The plasma sample (15 mL) after pooled was added 15 mL methanol and 15 mL acetonitrile and centrifugation (3,500 rpm, 10 min, 4°C). Extract the centrifuged solid with 7.5 mL water and 22.5 mL methanol acetonitrile (50:50, *v*: *v*). The first two extracted supernatants were combined and concentrated. The concentration of the substance is at 200 μL Acetonitrile water (20: 80, *v*: *v*) was dissolved again and centrifuged again (3,600 rpm, 10 min, 4°C). Part of the supernatant was injected into the UHPLC-FC (Fraction collector) system (Thermo). The eluent from the UHPLC was collected into the Deepwell LumaPlate 96 (PerkinElmer) at the rate of 10 s per well within minutes. The total collection time is

TABLE 2 Pharmacokinetic parameters of total radioactivity and SHR6390 in plasma after a single oral administration of [^{14}C]SHR6390 to healthy volunteers [mean (s.d.)].

Parameter	Unit	^{14}C plasma	SHR6390
C_{max}	ng eq./mL	167 (19.1)	42.9 (10.4)
AUC_{last}	ng eq./mL*h	1,670 (668)	1,150 (198)
AUC_{inf}	ng eq./mL*h	3,930 (1,250)	1,250 (206)
$t_{1/2}$	h	17.50 (7.92)	43.5 (7.77)
T_{max}	h	3.17 (1.83)	3.00 (1.79)

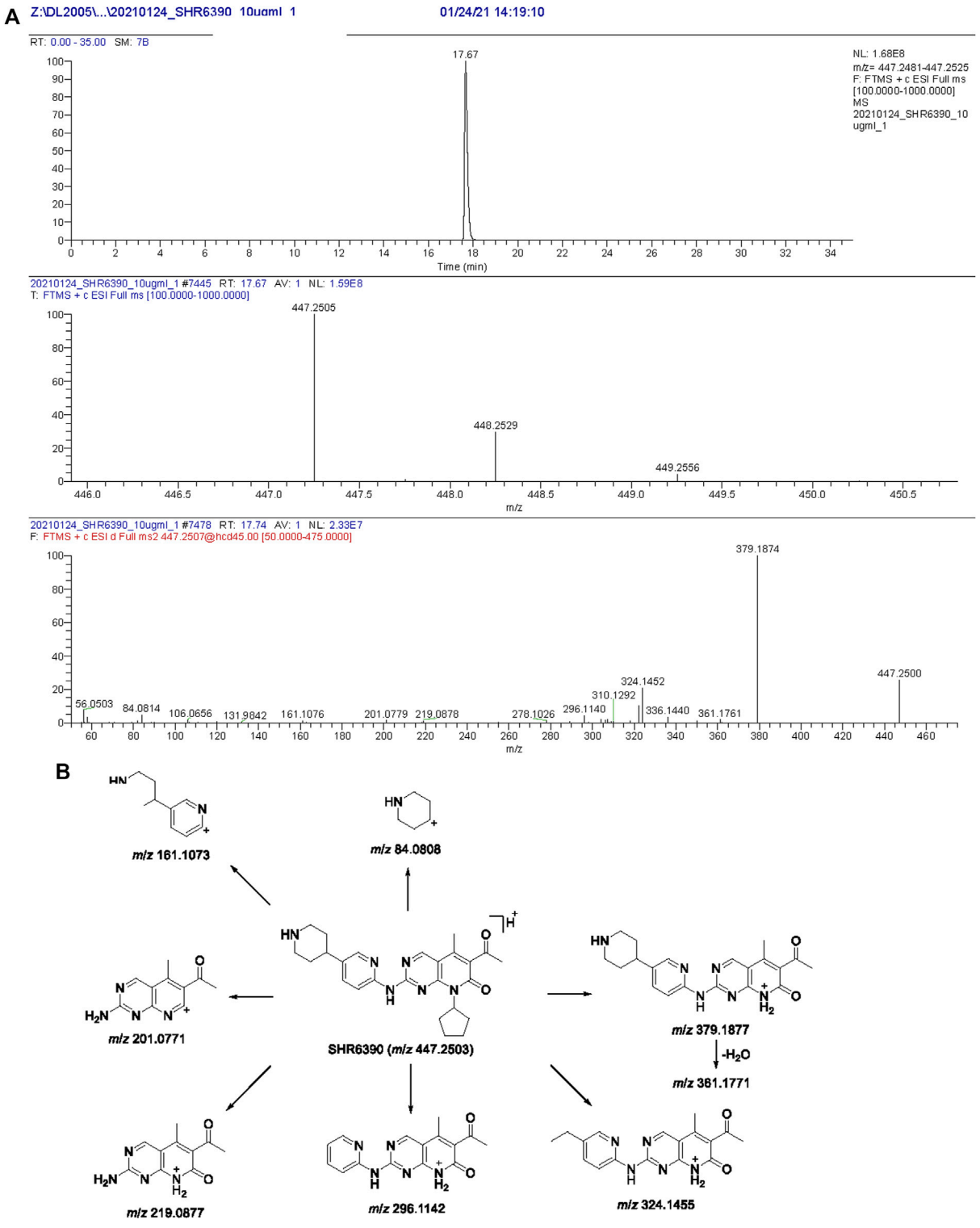

FIGURE 1
Extracted ion chromatograms, product ion spectra **(A)** and proposed fragmentation patterns of SHR6390 **(B)**.

35 min. The plates were dried by Integrated SpeedVac (Thermo), and the radiation value of each well were detected by a microplate reader (Sense Beta Hidex, Finland). Data were reconstructed to radio-chromatogram by Laura software (Lablogic, United Kingdom) to give the radio profiling of plasma.

2.5.3 Urine

According to the principle of equal volume, the urine samples of 6 subjects from 0 to 120 h were merged. The combined samples were centrifuged, concentrated by N_2 and dissolved in a 200 μL mixture of 40 mL acetonitrile and 160 mL-water, and 120 μL was injected into

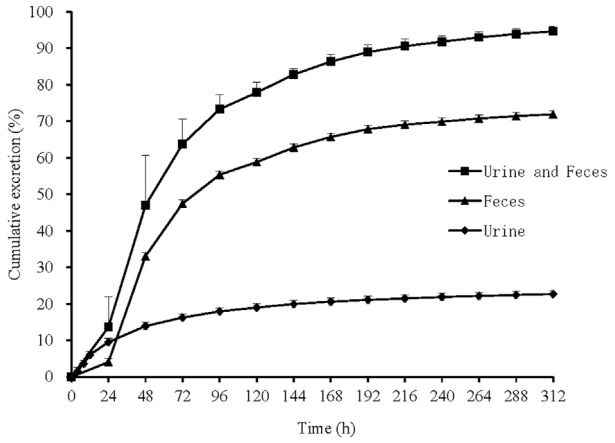

FIGURE 2
Mean cumulative excretion of total radioactivity in urine and feces following a single oral administration of [^{14}C]SHR6390. Each point represents the mean ± S.D. of six subjects.

the UHPLC-FC system (Thermo). Other operation steps are the same as those of plasma.

2.5.4 Stool

According to the principle of equal proportion weight, the fecal homogenates of 6 subjects from 0 to 168 h were combined. Add 6 mL methanol acetonitrile (50:50, v: v) to the combined fecal homogenate (2 g) sample. The mixture was then whirled (1 min) and centrifuged6 (3,500 rpm, 10 min, 4°C). Transfer the supernatant into a clean tube, and then extract the extracted solid again with 2 mL water and 2 mL methanol and 2 mL acetonitrile. The two supernatants were combined, concentrated by N_2 at 25°C and dissolved in acetonitrile-water (20: 80, v: v) of 200 μL, and 60 μL was injected into the UHPLC-FC system (Thermo). Other operation steps are the same as those of plasma.

2.6 Metabolite identification

The MS signal of the metabolites were obtained through UHPLC-HRMS, and the metabolic pathway of the metabolite was speculated. Through the MSMS spectrum obtained, the structure of the metabolite was identified by comparing the mass spectrum fragment with the mass spectrum fragment produced by the parent compound.

2.7 Pharmacokinetic analysis

The application software Phoenix WinNonlin (Version 7.0; Pharsight Corporation, Mountain View, CA) used a non-compartment model to calculate the parameters related to drug metabolism in this experiment. The related pharmacokinetic parameters for radioactivity are summarized in Table 2. By measuring the concentration of radioactive drugs in urine and stool, calculate the radioactive excretion rate (dose percentage) of each sample collected.

3 Result

3.1 HR-MS analysis of SHR6390

Chromatographic and HR-MS fragmentation of SHR6390 was studied. The structural analysis of metabolites is based on the structural analysis of the parent drug. SHR6390, $C_{25}H_{30}O_2N_6{\cdot}C_2H_6O_4S$, with $[M + H]^+$ at *m/z* 447.2503 eluted at 17.67 min and showed product ions at *m/z* 84.0808, 161.1073, 201.0771, 219.0877, 296.1142, 324.1455, 361.1771 and 379.1877 (Figures 1A, B). The base peak ion at *m/z* 379.1877 was generated by N-C cleavage of cyclopentane; further neutralization of H_2O and C_3H_5N led to *m/z* 361.1771 and 324.1455, respectively. Based on the peak ion, *m/z* 379.1877 underwent further N-C cleavages, generating *m/z* 219.0877 and 201.0771.

3.2 Pharmacokinetics

The radioactivity concentration-time profiles, the C_{max} of radioactivity was 166 ng eq./mL. The mean AUC_{last} value was 1,670 ng eq./mL*h. The mean T_{max} and $t_{1/2}$ were approximately 3.17 and 17.50 h, respectively. The radioactivity blood-to-plasma AUC_{inf} ratio (BPAR) of was 1.81. For SHR6390 in plasma, the mean C_{max} value of radioactivity was 42.9 ng/mL, and the mean AUC_{last} value was 1,150 ng/mL h. The mean AUC_{inf} values were 1,250 ng eq./mL*h. The mean T_{max} and $t_{1/2}$ were approximately 3.00 and 43.5 h, respectively.

3.3 Mass balance

In 6 healthy Chinese male subjects after an oral dose of 150 mg [^{14}C]SHR6390 (150 μCi), the recovery of total radioactivity was 94.63% (range 92.85%–96.34%). Stool excretion was the predominant route of elimination, accounting for 71.93% of the administered dose, while the mean urinary excretion was 22.69%. The total recovery in urine and stool in radioactive, 312 h after dosing was 94.63% (Figure 2).

3.4 Quantitative metabolite profiling

Radio-chromatograms of each matrix are shown in Figure 3. Table 3 summarizes some characteristics of 13 metabolites, from which the structure identification of metabolites can also be confirmed. The naming rule of metabolites is 'M + molecular weight.

3.4.1 Plasma

In AUC-pooled 0–24 h plasma, only SHR6390 was detected (Figure 3). The main reason was that the radioactivity in plasma was too low, and the signals of metabolites could not be distinguished from the background signal.

3.4.2 Urine

In the 0–120 h pooled urine sample, a total of 6 radio-chromatographic peaks were identified, and the major peak was the parent SHR6390 (Figure 3), accounting for 14.11% of the dose.

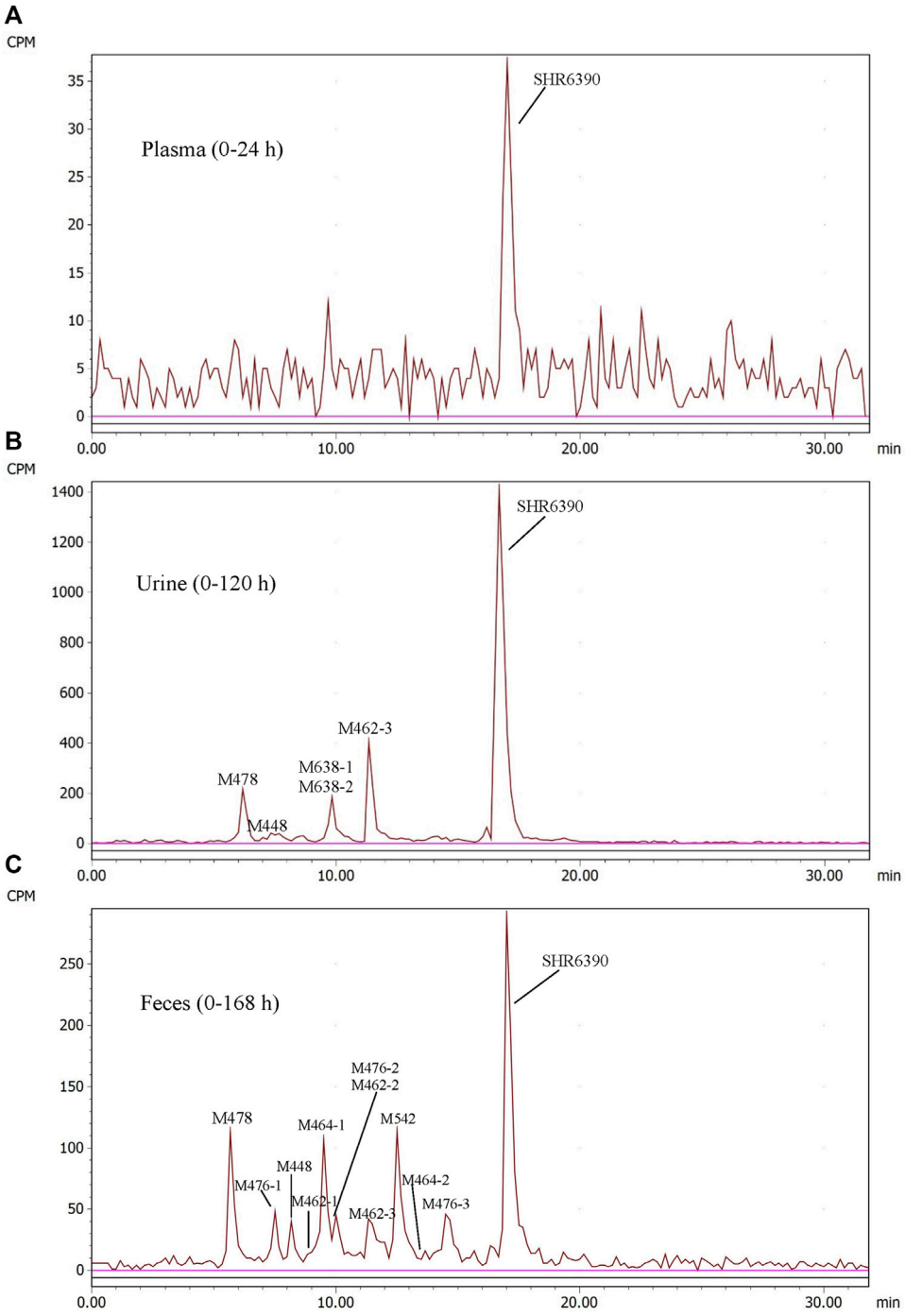

FIGURE 3
Representative radio-chromatograms of metabolites in human plasma (0–24 h) **(A)**, urine (0–120 h) **(B)**, and feces (0–168 h) **(C)** following oral administration of 150 mg [^{14}C]SHR6390 (150 μCi).

Five metabolites were assigned as M478, M448, M638-1/M638-2 (coeluting) and M462-3, accounting for 1.53%, 0.63%, 1.55% and 2.95% of the dose, respectively.

M462-3: The signal of MS showed that the elemental change of M462-3 might be an oxygen atom more than SHR6390. The main fragment ions were *m/z* 120.0808, 217.0720, 294.0984, 322.1293, 334.1299, 377.1721 and 395.1826. Comparing the ion fragments with those of the parent, the structure of M464-1 was deduced, as shown in Figures 4A, B.

M478: The signal of MS showed that the elemental change of M478 might be di-oxidation of parent SHR6390. The main fragment ions were *m/z* 178.1339, 223.1553, 349.1770, 365.1721, 393.1670 and 411.1775. Comparing the ion fragments with those of the parent, the structure of M464-1 was deduced, as shown in Figures 4C, D.

TABLE 3 Information on SHR6390 metabolites detected in human plasma, urine, and stool.

ID	Metabolic pathway	Formula	Retention time (min)	$[M + H]^+$ (determined)	Mass error (ppm)	Fragment ions
SHR6390	Parent	$C_{25}H_{30}O_2N_6$	16.67–17.00	447.2510	1.7	379.1847, 324.1452, 296.1140, 219.0878, 201.0779, 161.1076
M478	2[O]	$C_{25}H_{30}O_4N_6$	5.20–6.00	479.2410	1.8	411.1775, 393.1670,365.1721, 349.1770, 223.1552, 178.1339
M476-1	2[O]+[-2H]	$C_{25}H_{28}O_4N_6$	7.53	477.2254	2.0	409.1617, 365.1720, 310.1296, 282.1354, 205.0731, 161.1074
M448	$[-CH_2]$+[O]	$C_{24}H_{28}O_3N_6$	7.33–8.20	449.2312	3.6	363.1561, 337.1768, 308.1144, 282.1346, 161.1072
M462-1	[O]	$C_{25}H_{30}O_3N_6$	8.87	463.2471	4.1	379.1875, 324.1453, 296.1141, 201.0771, 161.1078
M464-1	[O]+[2H]	$C_{25}H_{32}O_3N_6$	9.53	465.2621	2.8	379.1875, 324.1451, 296.1144, 161.1078
M638-1	[O]+[GluA]	$C_{31}H_{38}O_9N_6$	9.83	639.2781	1.3	463.2460, 395.1830, 377.1721, 294.0976, 217.0718, 161.1075
M638-2	[O]+[GluA]	$C_{31}H_{38}O_9N_6$		639.2780	1.1	463.2457, 395.1827, 294.0999, 203.1290, 84.0816
M462-2	[O]	$C_{25}H_{30}O_3N_6$	10.03	463.2465	2.8	379.1874, 324.1458, 296.1136, 120.0810, 86.0971
M476-2	2[O]+[-2H]	$C_{25}H_{28}O_4N_6$		477.2255	2.2	409.1615, 365.1721, 310.1299, 282.1349, 205.0722, 161.1073
M462-3	[O]	$C_{25}H_{30}O_3N_6$	11.33-11.37	463.2467	3.3	395.1824, 377.1719, 322.1293, 294.0984, 217.0726, 120.0811
M542	[O]+$[SO_3]$	$C_{25}H_{30}O_6N_6S$	12.53	543.2034	2.5	463.2452, 395.1829, 377.1718, 322.1296, 294.0986, 217.0718
M464-2	[O]+[-2H]	$C_{25}H_{32}O_3N_6$	13.87	465.2624	3.3	379.1876, 324.1459, 296.1145, 219.0884, 136.0757, 120.0810
M476-3	2[O]+[-2H]	$C_{25}H_{28}O_4N_6$	14.53	477.2264	3.4	393.1670, 322.1299, 120.0808

In addition, M448 and two mono-oxidation and phase II glucuronide acid conjugates (M638-1 and M638-2) were also detected as minor metabolites in urine.

3.4.3 Stool

Parent SHR6390 and 12 metabolites were identified in the pooled 0–168 h fecal samples (Figure 3). Among them, SHR6390 was the predominant component (16%), and three abundant metabolites, M478, M464-1 and M542, accounted for 7.16%, 7.07% and 9.03% of the dose, respectively.

M464-1: The signal of MS showed that the elemental change of M478 was di-oxidation of parent SHR6390. The main product ions were *m/z* 161.1073, 296.1142, 324.1455 and 379.1877,397.1983. Comparing the ion fragments with those of the parent, the structure of M464-1 was deduced, as shown in Figures 4E, F.

M478: The details are shown in the urine section above.

M542: The signal of MS showed that the elemental change of M542 might be mono-oxidation and sulfation of the parent SHR6390. The main product ions were *m/z* 217.0720, 294.0986, 322.1299, 377.1717, 395.1926 and 463.2452. Comparing the ion fragments with those of the parent, the structure of M464-1 was deduced, as shown in Figures 4G, H.

In addition, M448, M462-1, M462-2, M462-3, M464-2, M476-1, M476-2 and M476-3 were also identified in stool as minor metabolites.

4 Discussion

This study reported the mass balance study of [^{14}C]SHR6390 in human. After oral administration, 94.63% of the dosed radioactivity was recovered in urine and stool by 312 h post-dose, which indicated complete excretion, with 22.69% in urine and 71.93% in stool.

Based on high radioactivity recovery in sample extraction, the metabolite profiles were evaluated. A total of 13 metabolites were identified, and unchanged SHR6390 was the major metabolite in three matrix following an oral administration of [^{14}C]SHR6390. In plasma, because of the low level of radioactivity, only SHR6390 was detected in pooled $AUC_{0\text{-}24h}$ plasma. In urine and stool, SHR6390 was the major component; 5 and 12 metabolites were identified, respectively.

The proposed biotransformation pathway based on findings from the present metabolism study is shown in Figure 5. The major metabolic pathways might be oxidation, glucuronidation and sulfation. As shown in Figure 5, the most susceptible metabolic spot of SHR6390 is the methyl on pyridyl pyrimidine and methyl of the acetyl group. The product ions at *m/z* 322.1293 and 294.0986 were used as diagnostic ions to determine the location of metabolism by summarizing the MS^2 spectra of SHR6390 and the available reference standards for the main metabolites. This rule applies in most cases, with occasional exceptions.

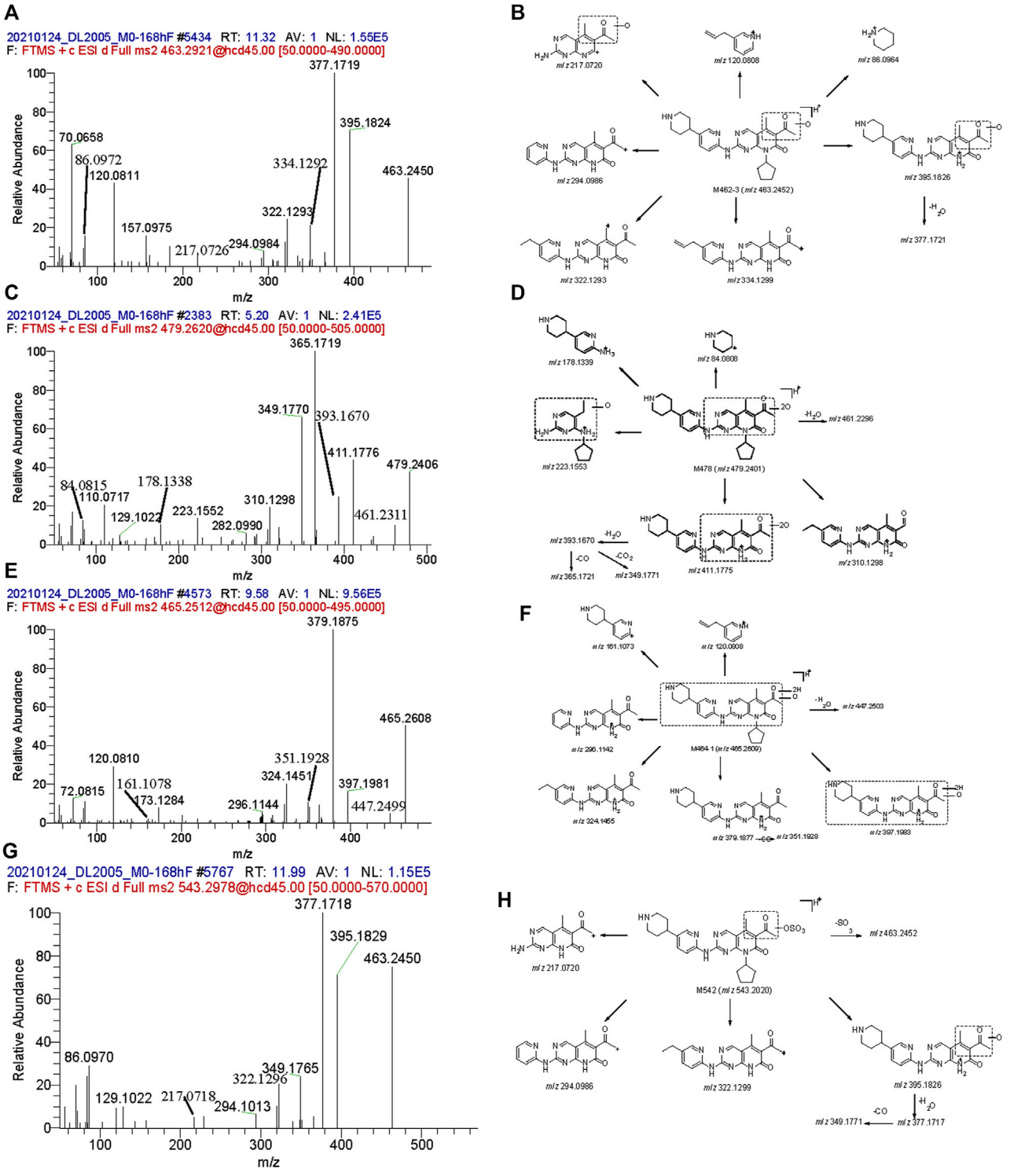

FIGURE 4
Mass spectra and the proposed fragmentation profiles of metabolites: M462-3 **(A, B)**, M478 **(C, D)**, M464-1 **(E, F)**, and M542 **(G, H)** in ESI (+).

In plasma, for the radioactivity concentration-time profiles, the mean C_{max} value of radioactivity was 166 ng eq/mL, and the mean AUC_{last} value was 1,670 ng eq./mL h. The mean T_{max} and $t_{1/2}$ were approximately 3.17 and 17.50 h, respectively. The blood-to-plasma AUC_{inf} ratio (BPAR) of the radioactivity was 1.81. For the observed blood-to-plasma ratio, it should be detected and identification the metabolites in blood to determine a more complete metabolic profiling. For SHR6390 in plasma, the mean Cmax value of radioactivity was 42.9 ng/mL, and the mean AUC_{0-t} value was 1,150 ng/mL h. The

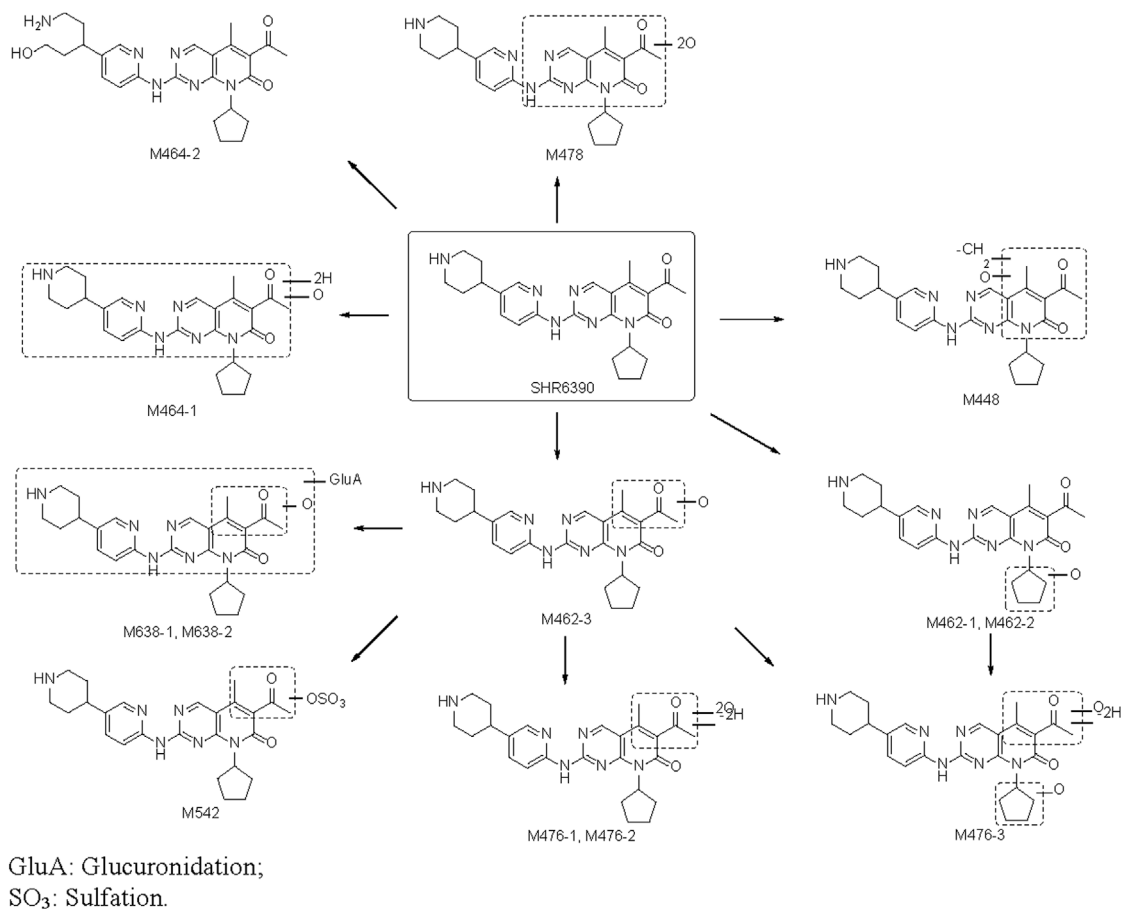

FIGURE 5
Metabolic pathway of SHR6390 in healthy Chinese male subjects.

mean $AUC_{0\text{-inf}}$ value was 1,250 ng/mL h. The mean T_{max} and $t_{1/2}$ were approximately 3.00 and 43.5 h, respectively.

Ribociclib was a medicine with similar structure. Concentrations of total radioactivity in blood and plasma were measured by AMS. The radioactivity mean $t_{1/2}$ in plasma of ribociclib were was 293 h. The mean C_{max} value of radioactivity was 1,140 ng eq/mL. The mean $AUC_{0\text{-inf}}$ value was 37,200 ng eq/mL*h (Alexander et al., 2020). The C_{max} and $AUC_{0\text{-inf}}$ of SHR6390 was lower. SHR6390 may have better activity. The differences in data do not fully explain the superiority of drugs, and may also be caused by differences in detection methods.

In conclusion, this study shows that after a single oral administration of [^{14}C] SHR6390, 94.63% of the dose was recovered in urine and feces, of which 22.69% was recovered in urine and 71.93% in feces. The characterization of SHR6390 pharmacokinetics, mass balance and metabolism is helpful to guide our understanding of SHR6290 metabolism and elimination pathway. In plasma, for the low level of radioactivity, only SHR6390 was detected in pooled $AUC_{0-24\ h}$ plasma. In urine and stool, SHR6390 was the major component; 5 and 12 metabolites were identified, respectively. Overall, faecal elimination played a significant role.

Data availability statement

The original contributions presented in the study are included in the article/supplementary material, further inquiries can be directed to the corresponding authors.

Ethics statement

The studies involving human participants were reviewed and approved by Ethics Committee of the First Affiliated Hospital of Soochow University. The patients/participants provided their written informed consent to participate in this study.

Author contributions

SY, JT, and YZ were responsible for the sample analysis; HZ, SY, LM, and XD were responsible for this manuscript; LM, XD, DZ, HZ, SY, SM, and GL designed the clinical study scheme and recruited volunteers; Jiangsu Hengrui Medicine Co., Ltd. offered the test drug and financial support.

Funding

This study was funded by Jiangsu Hengrui Pharmaceutical Co., Ltd. (Limited Company), and part of the funding was from the National Natural Science Foundation of China (81903701). This work was also supported by the national key new drug creation project (2017ZX09304-021), Suzhou Key Laboratory of Clinical Research and Personalized Medicine (SZS201719) and the special research fund of Wu Jieping Medical Foundation of Clinical Pharmacy Branch of Chinese Medical Association (320.6750.19090-50).

Conflict of interest

Authors SL and GL were employed by Jiangsu Hengrui Medicine Co., Ltd.

The remaining authors declare that the research was conducted in the absence of any commercial or financial relationships that could be construed as a potential conflict of interest.

Publisher's note

References

Alexander, D. J., Hilmar, S., Cyrille, M., Yi, J., Hubert, B., Ulrike, G., et al. (2020). An integrated assessment of the ADME properties of the CDK4/6 Inhibitor ribociclib utilizing preclinical *in vitro*, *in vivo*, and human ADME data. *Pharmacol. Res. Perspec* 8 (3), e00599. doi:10.1002/prp2.599

Arnold, A., and Papanikolaou, A. (2005). Cyclin D1 in breast cancer pathogenesis. *J. Clin. Oncol.* 23, 4215–4224. doi:10.1200/jco.2005.05.064

Asghar, U., Witkiewicz, A. K., Turner, N. C., and Knudsen, E. S. (2015). The history and future of targeting cyclin-dependent kinases in cancer therapy. *Nat. Rev. Drug Discov.* 14, 130–146. doi:10.1038/nrd4504

Bartkova, J., Lukas, J., Guldberg, P., Alsner, J., Kirkin, A. F., Zeuthen, J., et al. (1996). The p16-cyclin D/Cdk4-pRb pathway as a functional unit frequently altered in melanoma pathogenesis. *Cancer Res.* 56, 5475–5483.

Bian, Y., Zhang, H., Ma, S., Jiao, Y., Yan, P., Liu, X., et al. (2021). Mass balance, pharmacokinetics and pharmacodynamics of intravenous HSK3486, a novel anaesthetic, administered to healthy subjects. *Br. J. Clin. Pharmacol.* 87, 93–105. doi:10.1111/bcp.14363

Cadoo, K. A., Gucalp, A., and Traina, T. A. (2014). Palbociclib: An evidence-based review of its potential in the treatment of breast cancer. *Breast cancer (Dove Med. Press)* 6, 123–133. doi:10.2147/bctt.S46725

Cancer Genome Atlas Network (2012). Comprehensive molecular portraits of human breast tumours. *Nature* 490, 61–70. doi:10.1038/nature11412

Chen, Z., Xu, Y., Gong, J., Kou, F., Zhang, M., Tian, T., et al. (2020). Pyrotinib combined with CDK4/6 inhibitor in HER2-positive metastatic gastric cancer: A promising strategy from avatar mouse to patients. *Clin. Transl. Med.* 10, e148. doi:10.1002/ctm2.148

de Dueñas, E. M., Gavila-Gregori, J., Olmos-Antón, S., Santaballa-Bertrán, A., Lluch-Hernández, A., Espinal-Domínguez, E. J., et al. (2018). Preclinical and clinical development of palbociclib and future perspectives. *Clin. Transl. Oncol.* 20, 1136–1144. doi:10.1007/s12094-018-1850-3

Gelbert, L. M., Cai, S., Lin, X., Sanchez-Martinez, C., Del Prado, M., Lallena, M. J., et al. (2014). Preclinical characterization of the CDK4/6 inhibitor LY2835219: *In-vivo* cell cycle-dependent/independent anti-tumor activities alone/in combination with gemcitabine. *Invest. New Drugs* 32, 825–837. doi:10.1007/s10637-014-0120-7

Hartwell, L. H., Culotti, J., Pringle, J. R., and Reid, B. J. (1974). Genetic control of the cell division cycle in yeast. *Science* 183, 46–51. doi:10.1126/science.183.4120.46

Hop, C. E., Wang, Z., Chen, Q., and Kwei, G. (1998). Plasma-pooling methods to increase throughput for *in vivo* pharmacokinetic screening. *J. Pharm. Sci.* 87, 901–903. doi:10.1021/js970486q

Lappin, G. (2015). A historical perspective on radioisotopic tracers in metabolism and biochemistry. *Bioanalysis* 7, 531–540. doi:10.4155/bio.14.286

Long, F., He, Y., Fu, H., Li, Y., Bao, X., Wang, Q., et al. (2019). Preclinical characterization of SHR6390, a novel CDK 4/6 inhibitor, *in vitro* and in human tumor xenograft models. *Cancer Sci.* 110, 1420–1430. doi:10.1111/cas.13957

Lundberg, A. S., and Weinberg, R. A. (1998). Functional inactivation of the retinoblastoma protein requires sequential modification by at least two distinct cyclin-cdk complexes. *Mol. Cell. Biol.* 18, 753–761. doi:10.1128/mcb.18.2.753

Malumbres, M., and Barbacid, M. (2001). To cycle or not to cycle: A critical decision in cancer. *Nat. Rev. Cancer* 1, 222–231. doi:10.1038/35106065

Meng, J., Liu, X. Y., Ma, S., Zhang, H., Yu, S. D., Zhang, Y. F., et al. (2019). Metabolism and disposition of pyrotinib in healthy male volunteers: Covalent binding with human plasma protein. *Acta Pharmacol. Sin.* 40, 980–988. doi:10.1038/s41401-018-0176-6

Ming Yao, T. C., Duchoslav, E., Ma, L., Guo, X., Zhu, M., and Zhu, M. (2020). Software-aided detection and structural characterization of cyclic peptide metabolites in biological matrix by high-resolution mass spectrometry. *J. Pharm. Analysis* 10, 240–246. doi:10.1016/j.jpha.2020.05.012

Morgan, D. O. (1997). Cyclin-dependent kinases: Engines, clocks, and microprocessors. *Annu. Rev. Cell. Dev. Biol.* 13, 261–291. doi:10.1146/annurev.cellbio.13.1.261

Murai, T., Takakusa, H., Nakai, D., Kamiyama, E., Taira, T., Kimura, T., et al. (2014). Metabolism and disposition of [(14)C]tivantinib after oral administration to humans, dogs and rats. *Xenobiotica* 44, 996–1008. doi:10.3109/00498254.2014.926572

Penner, N., Xu, L., and Prakash, C. (2012). Radiolabeled absorption, distribution, metabolism, and excretion studies in drug development: Why, when, and how? *Chem. Res. Toxicol.* 25, 513–531. doi:10.1021/tx300050f

Prakash, C., Fan, B., Altaf, S., Agresta, S., Liu, H., and Yang, H. (2019). Pharmacokinetics, absorption, metabolism, and excretion of [(14)C]ivosidenib (AG-120) in healthy male subjects. *Cancer Chemother. Pharmacol.* 83, 837–848. doi:10.1007/s00280-019-03793-7

Robison, T. W., and Jacobs, A. (2009). Metabolites in safety testing. *Bioanalysis* 1, 1193–1200. doi:10.4155/bio.09.98

Shapiro, G. I. (2006). Cyclin-dependent kinase pathways as targets for cancer treatment. *J. Clin. Oncol.* 24, 1770–1783. doi:10.1200/jco.2005.03.7689

Tian, J., Lei, P., He, Y., Zhang, N., Ge, X., Luo, L., et al. (2021). Absorption, distribution, metabolism, and excretion of [14C]NBP (3-n-butylphthalide) in rats. *J. Chromatogr. B* 1181, 122915. doi:10.1016/j.jchromb.2021.122915

Wang, J., Li, Q., Yuan, J., Wang, J., Chen, Z., Liu, Z., et al. (2017). CDK4/6 inhibitor-SHR6390 exerts potent antitumor activity in esophageal squamous cell carcinoma by inhibiting phosphorylated Rb and inducing G1 cell cycle arrest. *J. Transl. Med.* 15, 127. doi:10.1186/s12967-017-1231-7

Weinberg, R. A. (1995). The retinoblastoma protein and cell cycle control. *Cell.* 81, 323–330. doi:10.1016/0092-8674(95)90385-2

Witkiewicz, A. K., and Knudsen, E. S. (2014). Retinoblastoma tumor suppressor pathway in breast cancer: Prognosis, precision medicine, and therapeutic interventions. *Breast Cancer Res.* 16, 207. doi:10.1186/bcr3652

Yamada, M., Mendell, J., Takakusa, H., Shimizu, T., and Ando, O. (2019). Pharmacokinetics, metabolism, and excretion of [(14)C]esaxerenone, a novel mineralocorticoid receptor blocker in humans. *Drug Metab. Dispos.* 47, 340–349. doi:10.1124/dmd.118.084897

Zhang, H., Ma, L., He, K., and Zhu, M. (2008). An algorithm for thorough background subtraction from high-resolution LC/MS data: Application to the detection of troglitazone metabolites in rat plasma, bile, and urine. *J. Mass Spectrom.* 43, 1191–1200. doi:10.1002/jms.1432

Zhang, H., Zhang, D., Ray, K., and Zhu, M. (2009). Mass defect filter technique and its applications to drug metabolite identification by high-resolution mass spectrometry. *J. Mass Spectrom.* 44, 999–1016. doi:10.1002/jms.1610

Zhang, P., Xu, B., Gui, L., Wang, W., Xiu, M., Zhang, X., et al. (2021). A phase 1 study of dalpiciclib, a cyclin-dependent kinase 4/6 inhibitor in Chinese patients with advanced breast cancer. *Biomark. Res.* 9, 24. doi:10.1186/s40364-021-00271-2

Zheng, Y. D., Zhang, H., Zhan, Y., Bian, Y. C., Ma, S., Gan, H. X., et al. (2021). Pharmacokinetics, mass balance, and metabolism of [(14)C]vicagrel, a novel irreversible P2Y(12) inhibitor in humans. *Acta Pharmacol. Sin.* 42, 1535–1546. doi:10.1038/s41401-020-00547-7